Supporting Information

Wier et al. 10.1073/pnas.1314754110

SI Materials and Methods

Protein Expression and Purification. The coding sequence for the human restores TBP function 1 (Rtf1) Plus3 domain (amino acids 353–484) was amplified from a full-length construct (kindly provided by R. Roeder, The Rockefeller University, New York) and subcloned into the pLC3 bacterial expression vector (J. Sacchettini, Texas A&M University, College Station, TX). The resulting vector expresses the Plus3 domain tagged with N-terminal His_6- and maltose binding protein (MBP)-tags, both of which can be removed via digestion with tobacco etch virus (TEV) protease. Plus3 protein was expressed using *Escherichia coli* Codon+ (RIPL) cells (Agilent Technologies) grown in ZY autoinduction media (1) at room temperature for 16–24 h. Cells were harvested by centrifugation, lysed with homogenization in 20 mM Tris (pH 8.0), 500 mM NaCl, 10% (vol/vol) glycerol, 5 mM Imidazole, and 1 mM β-mercaptoethanol, and the lysates were cleared by centrifugation at 30,000 × *g*. Plus3 protein was purified by nickel affinity chromatography (Qiagen) followed by an overnight digestion with TEV protease. After digestion, any uncleaved protein, His_6-MBP tag, and His_6-tagged TEV protease were removed by a second round of nickel affinity chromatography. The protein was then dialyzed at 4 °C overnight against a buffer containing 20 mM Tris pH 8.0, 20 mM NaCl, 8% glycerol, and 1 mM β-mercaptoethanol before cation exchange chromatography and gel filtration using a Sephacryl S-200 column (GE Healthcare). Peak fractions were concentrated to 8.5 mg/mL in 10 mM Hepes (pH 7.6), 80 mM NaCl, and 1 mM β-mercaptoethanol using a Vivaspin concentrator (Millipore) before crystallization.

Plasmids expressing mutant Plus3 proteins were generated by site-directed mutagenesis (QuikChange-Stratagene), and the resulting protein was expressed and purified in a manner similar to WT. After purification, Plus3 variants were concentrated to 6.0 mg/mL in 20 mM Tris pH 8.0, 100 mM NaCl, 5% glycerol, and 1 mM β-mercaptoethanol using a Vivaspin concentrator for use in differential scanning fluorimetry and fluorescence anisotropy assays. All peptides were synthesized at the University of Pittsburgh Peptide Synthesis Core.

Crystallization and Structure Determination. Plus3 crystals were grown at room temperature over 1–2 wk using the sitting drop vapor diffusion method against a reservoir solution containing 0.1 M sodium citrate pH 5.5 and 18% (wt/vol) polyethylene glycol (PEG3000). Crystals were cryoprotected by transition of the crystal into reservoir solution supplemented to 26% PEG3000 and 20% glycerol followed by flash freezing with liquid nitrogen. Crystals of the Plus3 domain in complex with a phosphorylated CTR peptide (pCTR) were generated by mixing Plus3 at 7.0 mg/mL with a fivefold molar excess of pCTR peptide and crystallized using sitting drop vapor diffusion as before using a reservoir solution containing 0.1 M sodium acetate pH 4.2 and 2.0 M ammonium sulfate. Crystals were grown at room temperature over a 2-wk period and were optimized using microseeding. Crystals were cryoprotected by transitioning the crystal into mother liquor supplemented to 3.5 M ammonium sulfate and flash freezing under liquid nitrogen.

Diffraction data for Plus3 crystals were collected at our home source, using an FR-E rotating anode generator with VariMax optics and RAXIS IV ++ image plate detector. Diffraction data were integrated, scaled, and merged using HKL2000 (2). Crystals of human Plus3 belong to the space group $P2_12_12_1$ (a = 33.6 Å, b = 68.0 Å, c = 117.0 Å; α = β = γ = 90.0°) and contain two molecules in the asymmetric unit. Initial phases were estimated via molecular replacement using Phaser (3), and a search model was derived from structural analysis of the Plus3 domain by NMR (4). The model was then refined against data to 2.12-Å resolution and improved by manual rebuilding within Coot (5) combined with simulated annealing, positional, B factor, and TLS refinement (6) within Phenix (7).

Diffraction data for Plus3–pCTR crystals were collected at the National Synchrotron Light Source on beamline ×25 using a Pilatus 6M detector. Plus3–pCTR crystals belong to the space group $C2_1$ (a = 112.9 Å, b = 172.5 Å, c = 58.5 Å; β = 107.0°) and contain six Rtf1 molecules in the asymmetric unit. Phases were determined using molecular replacement with Phaser but using our Plus3 structure as a starting model. Refinement restraints for the phosphothreonine residues were generated using eLBOW routine (8) as implemented in Phenix. The model was refined against diffraction data at 2.4-Å resolution and improved through the use of simulated annealing and refinement using positional, B factor, TLS, and noncrystallographic symmetry parameters. Model quality for both structures were assessed using MolProbity (9). All structural figures were generated using PyMol (PyMOL Molecular Graphics System, Version 1.5.0.4, Schrödinger, LLC.).

Models and structure factors for both the human Rtf1 Plus3 domain and the Plus3–pCTR complex presented in this manuscript have been deposited in Protein Data Bank (www.pdb.org) under the codes 4L1P and 4L1U.

Fluorescence Anisotropy. Purified Plus3 was titrated into a 400-μL reaction (10 mM Hepes, 50 mM NaCl) containing 20 nM fluorescein-labeled peptide (pCTR or CTR) and equilibrated for 2.5 min before measuring its anisotropic signal. Binding titrations were performed in triplicate, and average values and SD for each measurement were calculated. The Plus3-peptide dissociation constants (K_d) were determined in Prism (GraphPad) using nonlinear regression analysis. Titrations of Plus3 variants were carried out as above using a reaction buffer containing 100 mM NaCl.

Yeast Strain, Growth Media, and Plasmids. Experiments involving *Saccharomyces cerevisiae* were performed with strain KY619 (*MAT***a** *rtf1Δ102::ARG4 arg4-12 his4-912δ leu2Δ1 lys2-173R2 trp1Δ63*) and KY2417 (*MAT***α** *rtf1Δ::LEU2 cdc73Δ::KanMx his3Δ200 leu2Δ1 ura3(Δ0 or 52) trp1Δ63*), derivatives of FY2, a $GAL2^+$ derivative of S288C (10). Rich (YPD) and synthetic complete (SC) media for growth of yeast were prepared as previously described (11).

Plasmids pLS20 and pLS21-5 (12) express untagged and functional hemagglutinin (HA)-tagged Rtf1 (triple HA tag at the N terminus; HA_3-Rtf1), respectively, under the control of the *RTF1* promoter on *TRP1*-marked *CEN/ARS* plasmids. The *TRP1*-marked plasmids encoding the indicated HA_3-tagged mutant derivatives of Rtf1 were made using the Quickchange site-directed mutagenesis kit (Agilent) and pLS21-5 as the template. The *URA3*-marked plasmids expressing untagged mutant versions of Rtf1 were made by first removing the HA_3 tag from plasmids that express HA_3-Rtf1 by NdeI digestion and then ligating the XhoI-SacI fragment from these plasmids, containing the *RTF1* promoter and coding region, to pRS316 digested with XhoI-SacI. pMM61 and pMM62 (13) express untagged Rtf1 and Rtf1 lacking the Plus3 domain, under the control of the *RTF1* promoter on a *URA3*-marked *CEN/ARS* plasmids. pMM65 was generated using a QuikChange site-directed mutagenesis kit to introduce the R251A and Y327A substitutions in the Rtf1 protein. pCD3, pWR4

and pCD8 express untagged Cdc73, HA-tagged Cdc73 and HA-tagged Cdc73 lacking the C domain (14), respectively.

Western Blot Analysis. Trichloroacetic acid extracts were made from log-phase yeast cultures (OD_{600} 0.8–1.2) lysed by bead beating as described previously (15). Western blot analysis was performed as described previously (13) on extracts from strains expressing WT HA_3-Rtf1 or HA_3-Rtf1 derivatives containing the R251A, Y327A, and R251A/Y327A substitutions using antibodies against the HA epitope (1:2,500 dilution, Roche), Rtf1 (1:3,000 dilution) (16), Histone H3 K4 Me3 (1:2,000, Active motif 39159), H3 K4 Me2 (1:2,000, Upstate 07–030), H3 K79 Me2/3 (1:2,000, Abcam ab2621), H3 K36 Me3 (1:1,000, Abcam ab9050), total histone H3 (1:30,000) (15), or, as a loading control, glucose-6-phosphate dehydrogenase (1:30,000 dilution, Sigma A9521).

Chromatin Immunoprecipitation. Chromatin was prepared from log-phase cultures of the indicated yeast strains grown to a density of 1–2 × 10^7 cells/mL. Cells were treated with formaldehyde, quenched with glycine, harvested, and lysed as previously described (13). Chromatin was fragmented by sonication and incubated overnight at 4 °C with agarose-conjugated α-HA (Santa Cruz Biotechnology; sc-7392AC). Quantitative real-time PCR using Maxima SYBR Green/ROX qPCR master mix (Fermentas) and primers to the 5′ region of *PYK1* (+253 to +346, relative to the translation start codon ATG where A = +1), 5′ region of *PMA1* (+214 to +319), 3′ region of *PYK1* (+1127 to +1270), 3′ region of *PMA1* (+2107 to +2194), or telomeric region of chromosome VI (coordinates: 269495–269598) were used to determine the amount of *PYK1*, *PMA1*, or telomeric DNA associated with the HA-tagged proteins. The *y* axis of the graphs depicts the average values of the efficiency of the primer set$^{(\text{Ct of input})-(\text{Ct of IP})}$ for three biological replicates, and the error bars show the SEM.

1. Studier FW (2005) Protein production by auto-induction in high density shaking cultures. *Protein Expr Purif* 41(1):207–234.
2. Otwinowski Z, Minor W (1997) Processing of X-ray diffraction data collected in oscillation mode. *Methods Enzymol* 276:307–326.
3. McCoy AJ, et al. (2007) Phaser crystallographic software. *J Appl Cryst* 40(Pt 4):658–674.
4. de Jong RN, et al. (2008) Structure and DNA binding of the human Rtf1 Plus3 domain. *Structure* 16(1):149–159.
5. Emsley P, Lohkamp B, Scott WG, Cowtan K (2010) Features and development of Coot. *Acta Crystallogr D Biol Crystallogr* 66(Pt 4):486–501.
6. Zucker F, Champ PC, Merritt EA (2010) Validation of crystallographic models containing TLS or other descriptions of anisotropy. *Acta Crystallogr D Biol Crystallogr* 66(Pt 8):889–900.
7. Adams PD, et al. (2010) PHENIX: A comprehensive Python-based system for macromolecular structure solution. *Acta Crystallogr D Biol Crystallogr* 66(Pt 2):213–221.
8. Moriarty NW, Grosse-Kunstleve RW, Adams PD (2009) electronic Ligand Builder and Optimization Workbench (eLBOW): A tool for ligand coordinate and restraint generation. *Acta Crystallogr D Biol Crystallogr* 65(Pt 10):1074–1080.
9. Davis IW, et al. (2007) MolProbity: All-atom contacts and structure validation for proteins and nucleic acids. *Nucleic Acids Res* 35:W375–W383.
10. Winston F, Dollard C, Ricupero-Hovasse SL (1995) Construction of a set of convenient *Saccharomyces cerevisiae* strains that are isogenic to S288C. *Yeast* 11(1):53–55.
11. Rose MD, Winston F, Hieter P (1990) *Laboratory Course Manual for Methods in Yeast Genetics* (Cold Spring Harbor Laboratory, Cold Spring Harbor, New York).
12. Stolinski LA, Eisenmann DM, Arndt KM (1997) Identification of RTF1, a novel gene important for TATA site selection by TATA box-binding protein in *Saccharomyces cerevisiae*. *Mol Cell Biol* 17(8):4490–4500.
13. Mayekar MK, Gardner RG, Arndt KM (2013) The recruitment of the *Saccharomyces cerevisiae* Paf1 complex to active genes requires a domain of Rtf1 that directly interacts with the Spt4-Spt5 complex. *Mol Cell Biol* 33(16):3259–3273.
14. Amrich CG, et al. (2012) Cdc73 subunit of Paf1 complex contains C-terminal Ras-like domain that promotes association of Paf1 complex with chromatin. *J Biol Chem* 287(14):10863–10875.
15. Piro AS, Mayekar MK, Warner MH, Davis CP, Arndt KM (2012) Small region of Rtf1 protein can substitute for complete Paf1 complex in facilitating global histone H2B ubiquitylation in yeast. *Proc Natl Acad Sci USA* 109(27):10837–10842.
16. Squazzo SL, et al. (2002) The Paf1 complex physically and functionally associates with transcription elongation factors in vivo. *EMBO J* 21(7):1764–1774.

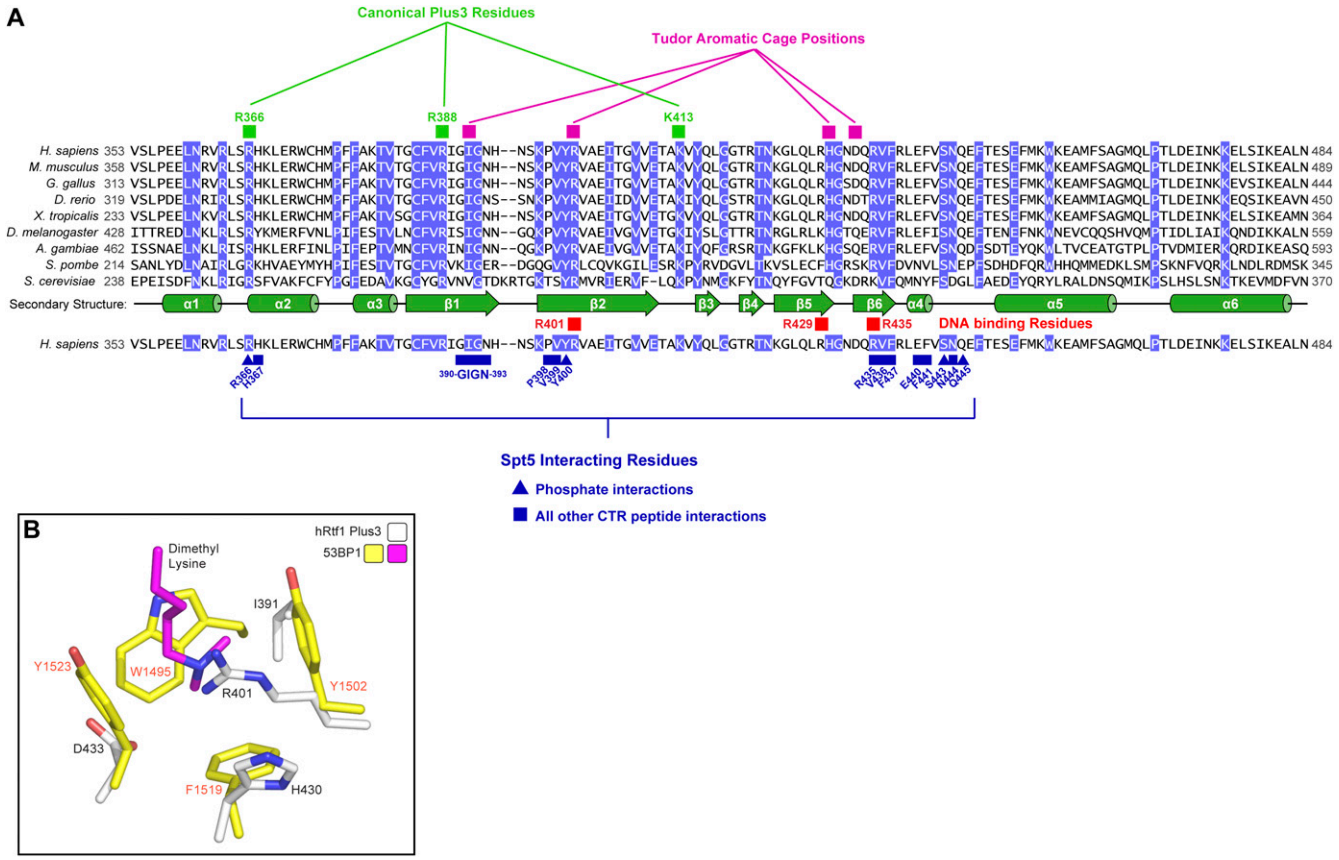

Fig. S1. Alignment of Rtf1 Plus3 sequences. (*A*) Multiple Rtf1 sequences were aligned using Clustal Omega and colored with Jalview at an identity cutoff of 85%. Invariant Plus3 residues (green) and positions that form the hydrophobic cage in Tudor domains (magenta) are indicated above the alignment. Rtf1 secondary structure observed in the Plus3-pCTR structure is indicated below the alignment, and residues making contacts with the Spt5 pCTR peptide are indicated (blue squares). Residues making direct hydrogen bonds with the pT784 are indicated (blue triangles). (*B*) Close-up of the methyl-binding aromatic cage from 53BP1 aligned to the Rtf1 Plus3 domain. Residues from 53BP1 (yellow), determined in complex with its ligand, dimethyl-lysine (magenta) (1), are indicated. The equivalent positions from the superposed Plus3-CTR complex are indicated in white.

1. Botuyan MV, et al. (2006) Structural basis for the methylation state-specific recognition of histone H4-K20 by 53BP1 and Crb2 in DNA repair. *Cell* 127(7):1361–1373.

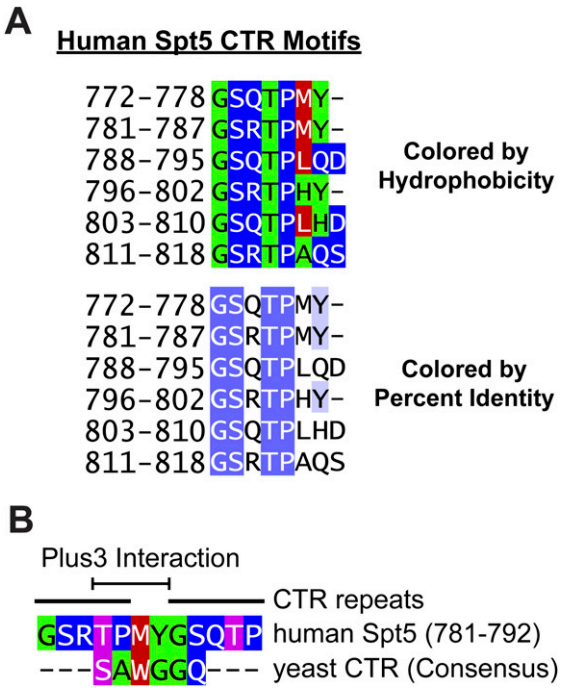

Fig. S2. Conservation within the human Spt5 CTR motif. (*A*) The six recognized CTR motifs from human Spt5 were aligned and colored by hydrophobicity (1) or identity, highlighting conservation of chemical properties among spacer residues. (*B*) Alignment of a consensus CTR from *S. cerevisae* (2) with a segment of human Spt5 (781–792) containing two CTR repeats. The alignment is anchored by the position of the phosphorylated residue (magenta), whereas the other residues are colored by hydrophobicity (1) as in *A*. Spt5 CTR residues that were observed to interact directly with the Rtf1 Plus3 domain are indicated.

1. Rose GD, Geselowitz AR, Lesser GJ, Lee RH, Zehfus MH (1985) Hydrophobicity of amino acid residues in globular proteins. *Science* 229(4716):834–838.
2. Liu Y, et al. (2009) Phosphorylation of the transcription elongation factor Spt5 by yeast Bur1 kinase stimulates recruitment of the PAF complex. *Mol Cell Biol* 29(17):4852–4863.

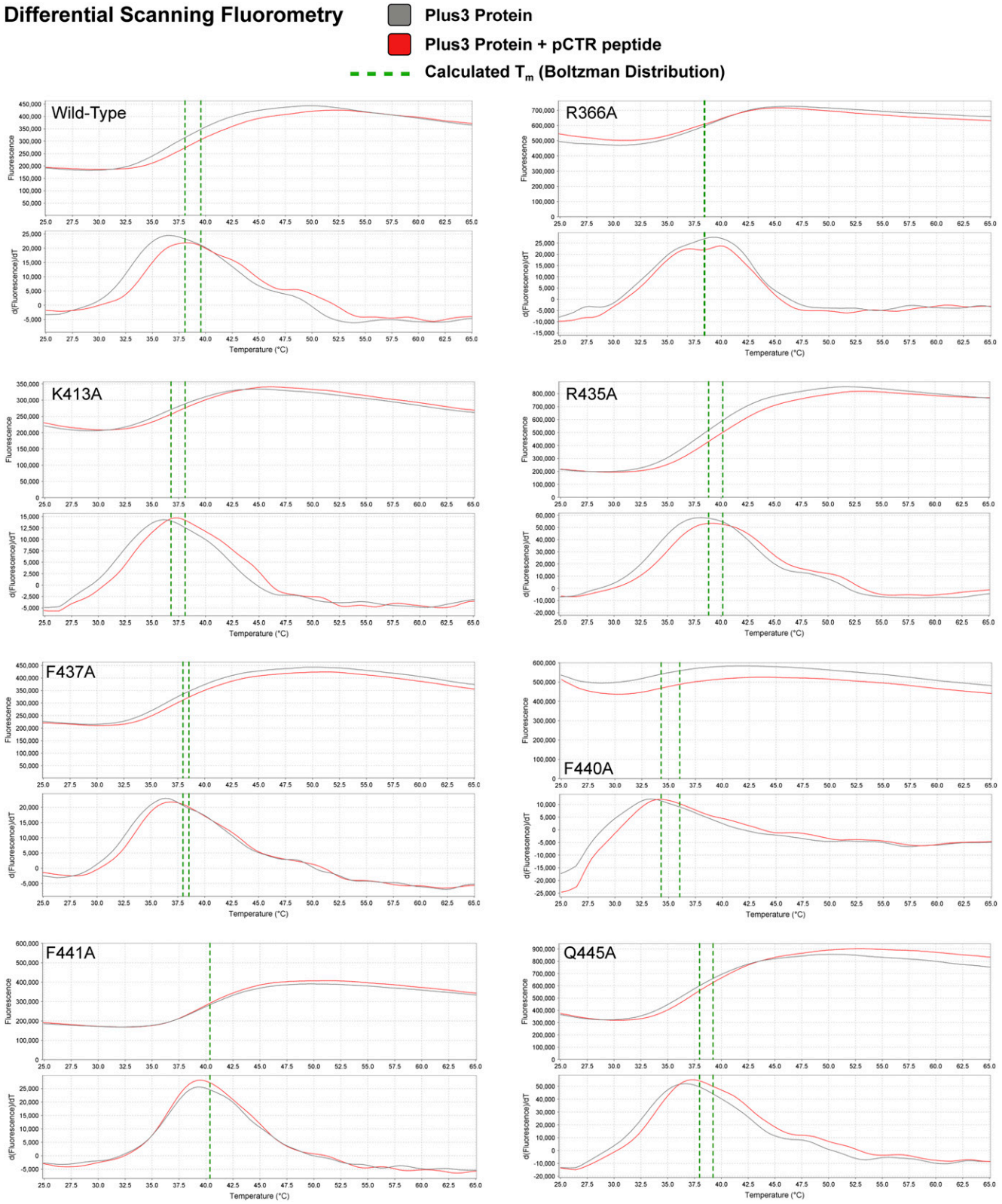

Fig. S3. Differential scanning fluorimetry analysis of human Rtf1 Spt5 pCTR interactions. Fluorescence intensity was measured for WT or the indicated Plus3 variant during the course of a melting curve. Representative curves from 12 independent replicates are shown for experiments with Plus3 protein alone (gray) or in the presence of peptide (red). The green dotted line represents the Boltzmann-derived melting temperature (T_m).

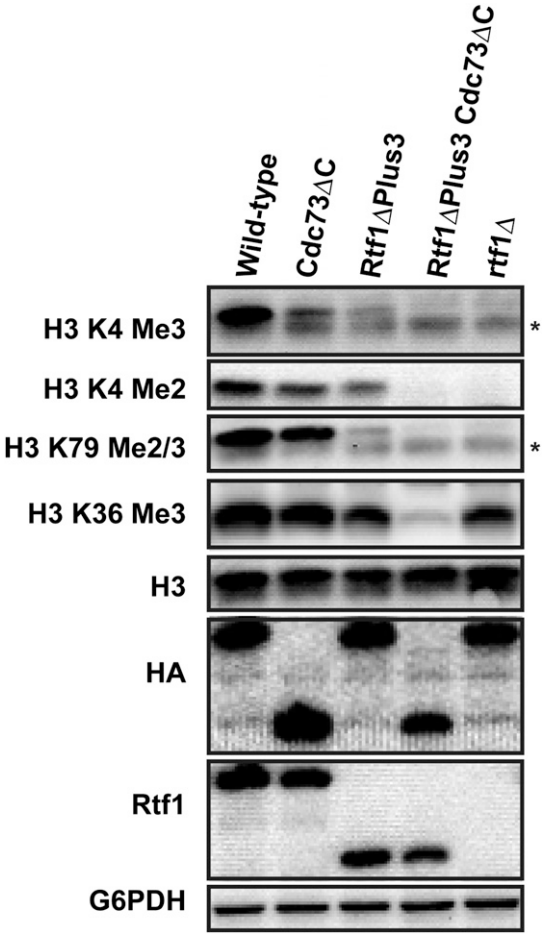

Fig. S4. The impact of deleting the Rtf1 Plus3 and Cdc73 C domains on histone modification levels. Western blot analysis was performed on transformants of an *rtf1*Δ*cdc73*Δ (KY2417) strain containing a plasmid expressing full-length HA-tagged Cdc73 (pWR4) or Cdc73ΔC (pCD8), and a plasmid encoding full-length Rtf1 (pMM61) or Rtf1ΔPlus3 (pMM62), or an empty vector (pRS316) using the indicated antibodies. Nonspecific bands are indicated by an asterisk.

Table S1. Crystallographic data collection and refinement statistics

	Human Rtf1 Plus3	Plus3-pCTR complex
Data collection		
Space group	P 2_1 2_1 2_1	C 2_1
Cell dimensions		
a, *b*, *c*; Å	33.6, 68.0, 117.0	112.9, 172.5, 58.48
α, β, γ; °	90.0, 90.0, 9.0	90.0, 107.0, 90.0
Unique reflections	14,681	40,278
Resolution, Å	50.0–2.12 (2.16–2.12)	50.0–2.43 (2.52–2.43)
R_{merge}, %	8.50 (62.4)	6.8 (37.6)
$I/\sigma I$	9.82 (2.60)	14.6 (2.31)
Completeness, %	91.9 (94.1)	99.9 (99.9)
Redundancy	4.6 (4.5)	3.6 (3.4)
Refinement		
Resolution, Å	29.2–2.12 (2.19–2.12)	46.9–2.42 (2.51–2.43)
R_{work}/R_{free}, %	20.6/24.0 (26.3/33.4)	17.7/22.4 (22.6/29.4)
No. of atoms		
Protein	2109	6484
Peptide		235
Solvent	101	280
B factors		
Protein	51.1	49.5
Peptide		69.2
Solvent	53.8	68.5
rmsd		
Bond lengths, Å	0.006	0.004
Bond angles, °	0.94	0.92
Ramachandrian, %		
Outliers	0.00	0.00
Allowed	1.19	1.74
Favored	98.8	98.3

Values in parentheses are for highest-resolution shell. $R_{merge} = [|(\Sigma I - \langle I \rangle)|]/(\Sigma I)$, where $\langle I \rangle$ is the average intensity of multiple measurements. $R_{work} = \Sigma_{hkl}||F_{obs}(hkl)|| - F_{calc}(hkl)||/\Sigma_{hkl}|F_{obs}(hkl)|$. R_{free} = crossvalidation R factor for a subset of reflections against which the model was not refined.